

Unexpected Evolution of Optical Properties in Ir-Pt Complexes Upon Repeat Unit Increase: Towards an Understanding of the Photophysical Behaviour of Organometallic Polymers

Ahmed M. Soliman, Daniel Fortin, Eli Zysman-Colman and Pierre D. Harvey**

*Département de chimie, Université de Sherbrooke,
2500 Boul. Université, Sherbrooke, QC, J1K 2R1*

Pierre.Harvey@usherbrooke.ca; Eli.Zysman-Colman@usherbrooke.ca

SUPPORTING INFORMATION

<u>Table of Contents:</u>	<u>Pages</u>
Experimental section	S2-S6
Absorption and emission spectra of individual complexes	S7-S10
Excitation and absorption at 77K	S11
Spectroscopic and photophysical data of 1, 2, 3, 6 and 7 in 2-MeTHF	S12
Cyclic voltammograms for 4, 2, 3, 7 and 6	S13
Energy and composition of TD-DFT calculated transitions for 7	S14
¹H, ¹³C and ³¹P NMR spectra of 7 and 11	S15-S20
References	S21

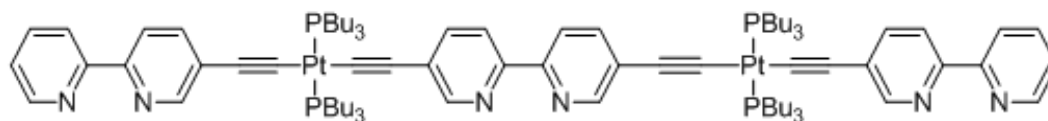
Experimental section

Synthesis:

General Procedures:

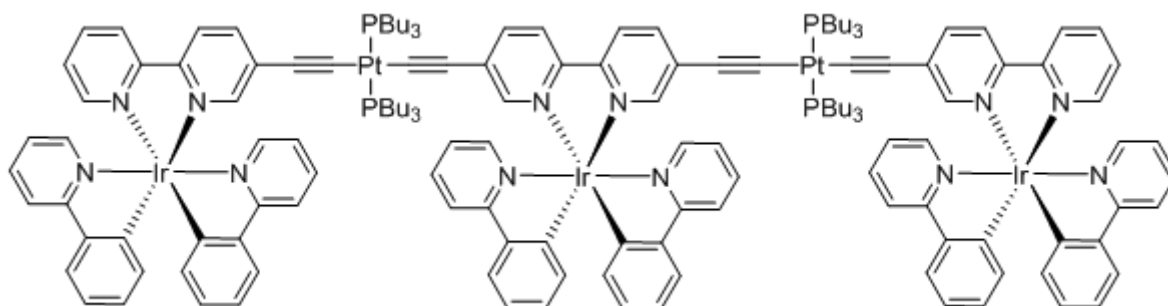
Commercial chemicals were used as supplied. All experiments were carried out with freshly distilled anhydrous solvents obtained from a Pure SolvTM solvent purification system from Innovative Technologies except where specifically mentioned. Triethylamine (Et₃N), *N,N*-diisopropylamine (*i*-Pr₂NH) were distilled over CaH₂ under a nitrogen atmosphere. PtCl₂(PBU₃)₂ was obtained following standard literature protocol¹ and heated to 165 °C to obtain the *trans* form. CuI,² [(ppy)₂Ir-μ-Cl]₂ dimer,³ 5,5'-diethynyl-2,2'-bipyridine (**10**)⁴ and *trans*-(5-ethynyl-2,2'-bipyridine)-chloro-bis(tri-*n*-butylphosphine)platinum (**9**)⁵ were purified or prepared following literature procedures. All reagents wherein the synthesis is not explicitly described in the SI were purchased and used without further purification. Flash column chromatography was performed using silica gel (Silica-P from Silicycle, 60 Å, 40-63 μm). Analytical thin layer chromatography (TLC) was performed with silica plates with aluminum backings (250 μm with indicator F-254). Compounds were visualized under UV light. ¹H and ¹³C NMR spectra were recorded on a Bruker Avance spectrometer at 400 MHz and 100 MHz, respectively or a Bruker Avance spectrometer at 300 MHz and 75MHz, respectively. ³¹P NMR spectra was recorded on a Bruker Avance spectrometer at 121 MHz and 162 MHz, respectively. The following abbreviations have been used for multiplicity assignments: "s" for singlet, "d" for doublet, "t" for triplet and "m" for multiplet. Deuterated chloroform (CDCl₃) and deuterated acetonitrile (CD₃CN) were used as the solvent of record. Melting points (Mp's) were recorded using open end capillaries on a Meltemp melting point apparatus and are uncorrected. GC-MS samples were separated on a Shimadzu QP 2010 Plus equipped with a HP5-MS 30 m x 0.25 mm ID x 0.25 μm film thickness column. High resolution mass spectra were recorded on either a VG Micromass ZAB-2F or a Waters Synapt MS G1 (ES-Q-TOF) at the Université de Sherbrooke.

Complex 11:



A dry flask charged with *trans*-(5-ethynyl-2,2'-bipyridine)-chloro-bis(tri-*n*-butylphosphine)platinum (**9**) (0.11 g, 0.15 mmol, 2.2 equiv.), CuI (9.0 mg, 0.05 mmol, 0.30 equiv.), DCM (40 mL) and *i*-Pr₂NH (15 mL) was purged with N₂ for 30 min. 5,5'-diethynyl-2,2'-bipyridine (**10**) (12.5 mg, 0.06 mmol, 1.0 equiv.), dissolved in DCM (10 mL), was then added. The mixture was stirred at room temperature for 20 h. The solvent was removed under reduced pressure and the residue was re-dissolved in DCM (30 mL). The organic phase was washed with H₂O twice then dried over MgSO₄ and concentrated under reduced pressure. The residue was purified by flash chromatography (10% EtOAc/Hexanes on silica gel) to yield 39 mg of yellow solid (Yield: 42%). **Rf**: 0.38 (10% EtOAc/Hexane). **Mp**: 202-204 °C. **¹H NMR (300 MHz, CDCl₃) δ (ppm)**: 8.66 (d, *J* = 4.8 Hz, 2H), 8.57 (dd, *J* = 7.5, 1.5 Hz, 4H), 8.34 (d, *J* = 8.0 Hz, 2H), 8.24 (d, *J* = 8.2 Hz, 2H), 8.19 (d, *J* = 8.3 Hz, 2H), 7.79 (td, *J* = 7.8, 1.6 Hz, 2H), 7.63 (td, *J* = 8.6, 2.0 Hz, 4H), 7.29 – 7.23 (m, 2H), 2.21 – 2.09 (m, 24), 1.70 – 1.52 (m, 24H), 1.53 – 1.36 (m, 24H), 0.93 (t, *J* = 7.2 Hz, 36H). **¹³C NMR (75 MHz, CDCl₃) δ (ppm)**: 156.24, 151.78, 151.61, 151.11, 149.13, 138.13, 138.12, 136.80, 125.72, 125.10, 123.14, 120.80, 120.20, 119.94, 106.43, 106.24, 26.34, 24.39, 23.92, 13.80. **³¹P NMR (121 MHz, CDCl₃) δ (ppm)**: 4.66 (d, *J* = 2330.5 Hz). **LR-MS (EI, 70eV) (*m/z*)**: 1760 (M⁺). **HR-MS (EI, 70eV): Calculated (C₈₆H₁₂₈N₆P₄Pt₂): 1760.8536; Found: 1760.8509.**

Complex 7:



The dimeric complex $[(ppy)_2Ir-\mu-Cl]_2$ (32 mg, 0.03 mmol, 2.5 equiv.) was dissolved in DCM (4 mL) and methanol (4 mL) and **11** (21 mg, 0.01 mmol, 1.0 equiv.) was added as a solid. The mixture was stirred at 60 °C for 24 h. The solution was cooled to RT and extracted with water (3 x 50 mL), then washed with ether (3 x 50 mL) to remove unreacted **11**. To the aqueous solution was slowly added a solution of NH_4PF_6 (10 mL, 10 % w/w in H_2O) under gentle stirring. The first drop caused the precipitation of a red solid. The suspension was conserved at 0 °C for 2 h and then filtered and the resulting solid was washed with cold water. The residue was purified by flash chromatography (10% MeOH/DCM on silica gel) to yield 30 mg of a red solid (Yield: 69%). **Rf**: 0.72 (10%MeOH/DCM). **Mp**: 195 °C (dec). **1H NMR (300 MHz, CD_3CN) δ (ppm)**: 8.42 (d, J = 8.0 Hz, 1H), 8.34 (d, J = 8.5 Hz, 1H), 8.24 (d, J = 8.6 Hz, 1H), 8.07 (dd, J = 7.9, 2.8 Hz, 7H), 7.95 (d, J = 5.3 Hz, 2H), 7.91 – 7.88 (m, 2H), 7.86 (s, 3H), 7.80 (dd, J = 7.1, 3.4 Hz, 9H), 7.76 (d, J = 0.7 Hz, 2H), 7.72 (d, J = 1.4 Hz, 2H), 7.63 (t, J = 5.6 Hz, 6H), 7.51 – 7.39 (m, 2H), 7.09 – 6.98 (m, 11H), 6.92 (t, J = 7.4 Hz, 6H), 6.30 – 6.23 (m, 5H), 5.98 – 5.77 (s, 8H), 1.82 (s, 24H), 1.34 (m, 48H), 0.77 (t, J = 7.2 Hz, 36H). **^{13}C NMR (75 MHz, CD_3CN) δ (ppm)**: 172.72, 172.54, 161.08, 157.12, 156.54, 155.93, 155.81, 155.58, 154.55, 154.41, 154.35, 149.30, 144.49, 144.41, 144.36, 143.83, 136.81, 135.78, 135.65, 132.95, 130.19, 129.56, 129.42, 129.07, 128.86, 128.73, 127.94, 127.80, 125.16, 125.11, 31.45, 29.31, 28.93, 18.38. **^{31}P NMR (121 MHz, CD_3CN) δ (ppm)**: 11.29 (d, J = 2271.0 Hz). **LR-MS (EI, 70eV) (m/z)**: 1087 (M^{3+}), 979, 501. **HR-MS (EI, 70eV): Calculated** ($C_{152}H_{176}F_{18}Ir_3N_{12}P_7Pt_2$): 1087.3760 (M^{3+}); **Found**: 1087.3791 (M^{3+}).

Photophysical characterization: All samples were prepared in 2-methyltetrahydrofuran (2-MeTHF), which was distilled over CaH_2 under nitrogen or HPLC grade acetonitrile (ACN) for the external reference. Absorption spectra were recorded at room temperature and at 77 K in a 1.0 cm capped quartz cuvette and an NMR tube inserted into a liquid nitrogen filled quartz dewar, respectively, using a Shimadzu UV-1800 double beam spectrophotometer. Molar absorptivity determination was verified by linear least squares fit of values obtained from at least three independent solutions at varying concentrations with absorbances ranging from 0.01-2.6. Steady-state emission spectra were obtained by exciting at the lowest energy absorption maxima using a Horiba Jobin Yvon Fluorolog-3 spectrofluorometer equipped with double monochromators and a photomultiplier tube detector (Hamamatsu model R955). Emission quantum yields were determined using the optically dilute method.^{6 7} A stock solution with absorbance of ca. 0.5 was prepared and then four dilutions were prepared with dilution factors of 40, 20, 13.3 and 10 to obtain solutions with absorbances of ca. 0.013,

0.025, 0.038 and 0.05, respectively. The Beer-Lambert law was found to be linear at the concentrations of the solutions. The emission spectra were then measured after the solutions were rigorously degassed with solvent-saturated nitrogen gas (N₂) for 20 minutes prior to spectrum acquisition using septa-sealed quartz cells from Starna. For each sample, linearity between absorption and emission intensity was verified through linear regression analysis and additional measurements were acquired until the Pearson regression factor (R^2) for the linear fit of the data set surpassed 0.9. Individual relative quantum yield values were calculated for each solution and the values reported represent the slope value. The equation $\Phi_s = \Phi_r(A_r/A_s)(I_s/I_r)(n_s/n_r)^2$ was used to calculate the relative quantum yield of each of the sample, where Φ_r is the absolute quantum yield of the reference, n is the refractive index of the solvent, A is the absorbance at the excitation wavelength, and I is the integrated area under the corrected emission curve. The subscripts s and r refer to the sample and reference, respectively. A solution of [Ru(bpy)₃](PF₆)₂ in ACN ($\Phi_r = 0.095\%$) was used as the external reference.⁸ The experimental uncertainty in the emission quantum yields is conservatively estimated to be 10%, though we have found that statistically we can reproduce PLQYs to 3% relative error. The emission lifetimes were measured on a TimeMaster model TM-3/2003 apparatus from PTI. The source was a nitrogen laser with high-resolution dye laser (fwhm ~1400 ps), and the excited state lifetimes were obtained from deconvolution or distribution lifetimes analysis. Some samples were also measured using a time-correlated single photon counting (TCSPC) option of the Jobin Yvon Fluorolog-3 spectrofluorometer, a pulsed NanoLED at 341 nm (pulse duration < 1 ns; fwhm = 14 nm), mounted directly on the sample chamber at 90° to the emission monochromator, was used to excite the samples and emitted light was collected using a FluoroHub from Horiba Jobin Yvon single-photon-counting detector. The luminescence lifetimes were obtained using the commercially available Horiba Jobin Yvon Decay Analysis Software version 6.4.1, software included within the spectrofluorimeter.

Computational Methodology. Calculations were performed with Gaussian 09⁹ at the Université de Sherbrooke with Mammouth super computer supported by Calcul Québec. The DFT¹⁰ and TDDFT¹¹ were calculated with the B3LYP¹² method. The 3-21G*¹³ basis set was used for C, H and N, and VDZ (valence double ζ) with SBKJC effective core potentials^{13a, 14} for iridium and platinum. The predicted phosphorescence wavelengths were obtained by energy differences between the Triplet and Singlet optimized states.¹⁵ The calculated absorption spectra and related MO contributions were obtained from the TD-DFT/Singlets

output file and gausssum 2.1.¹⁶ A THF quantum mechanical continuum solvation model was employed.¹⁷

Electrochemical Characterization. Cyclic voltammetry were performed on an Electrochemical Analyzer potentiostat model 600D from CH Instruments. Solutions for cyclic voltammetry were prepared in ACN and degassed with ACN-saturated nitrogen bubbling for ca. 15 min prior to scanning. Tetra(n-butyl)ammonium hexafluorophosphate (TBAPF₆; ca. 0.1 M in ACN) was used as the supporting electrolyte. It was recrystallized twice from EtOH and dried under vacuum prior to use. A non-aqueous Ag/Ag⁺ electrode (silver wire in a solution of 0.1 M AgNO₃ in ACN) was used as the pseudo-reference electrode; a glassy-carbon electrode was used for the working electrode and a Pt electrode was used as the counter electrode. The redox potentials are reported relative to a saturated calomel (SCE) electrode with a ferrocenium/ferrocene (Fc⁺/Fc) redox couple as an internal reference (0.40 V vs SCE).¹⁸

Figure S1: Absorption (green) and emission spectra at 298 K (red) and 77 K (blue) in 2-MeTHF for **11**:

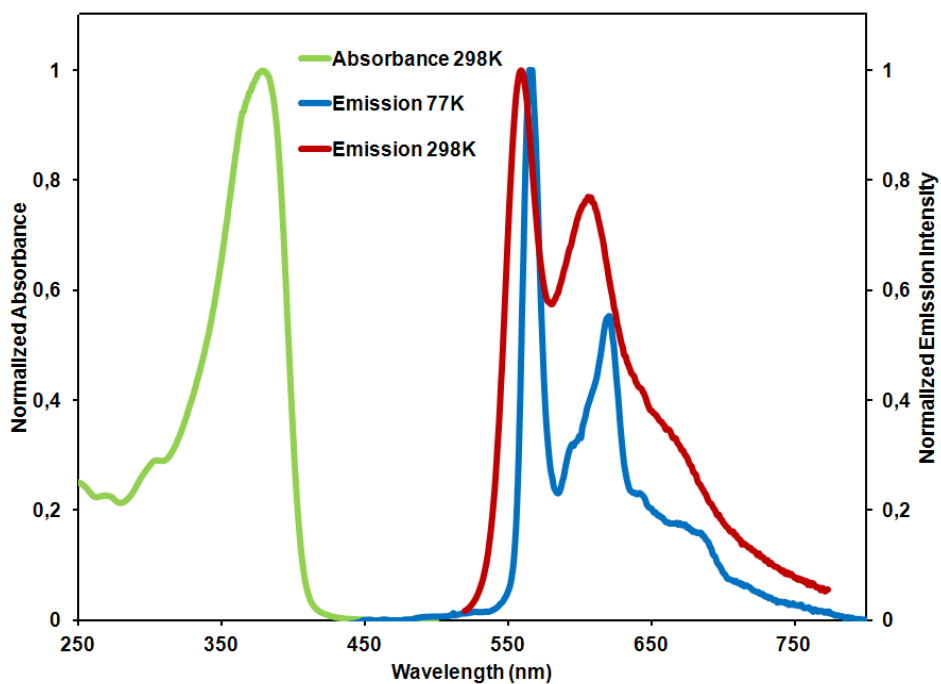


Figure S2: Absorption (green) and emission spectra at 298 K (red) and 77 K (blue) in 2-MeTHF for **7**:

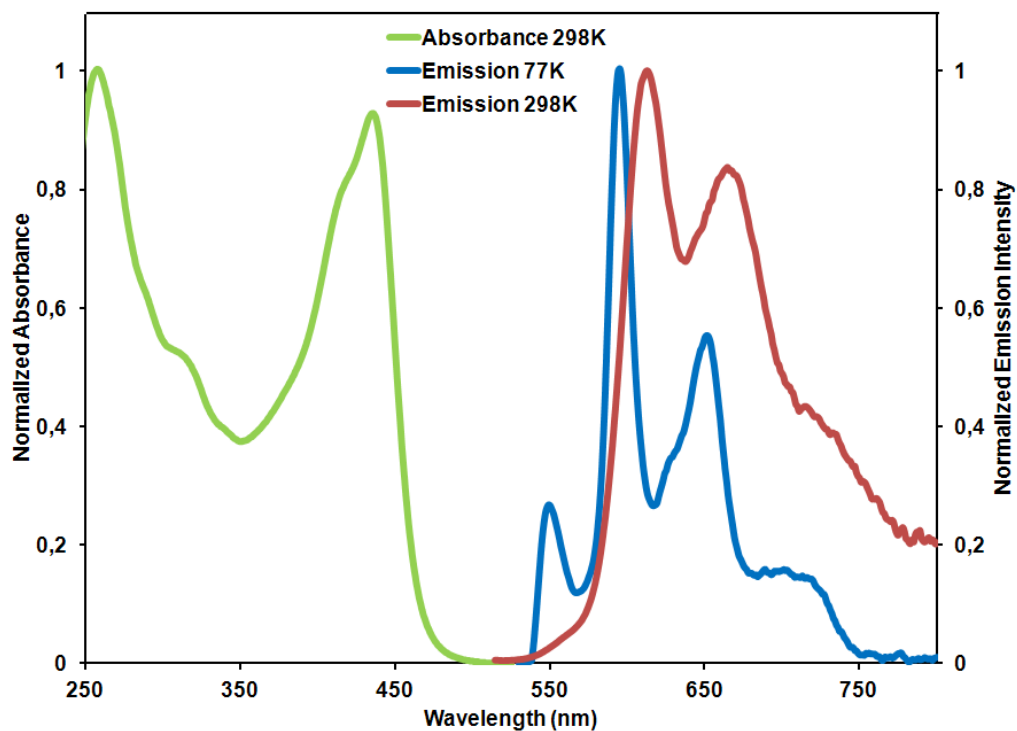


Figure S3: Absorption (green) and emission spectra at 298 K (red) and 77 K (blue) in 2-MeTHF for **1**:

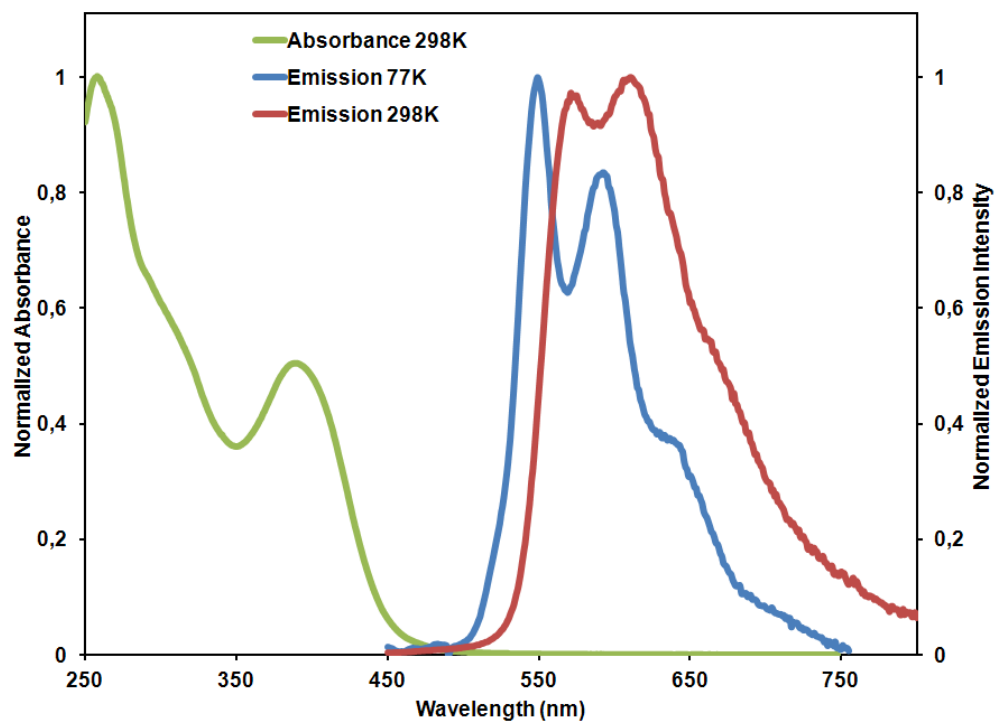


Figure S4: Absorption (green) and emission spectra at 298 K (red) and 77 K (blue) in 2-MeTHF for **2**:

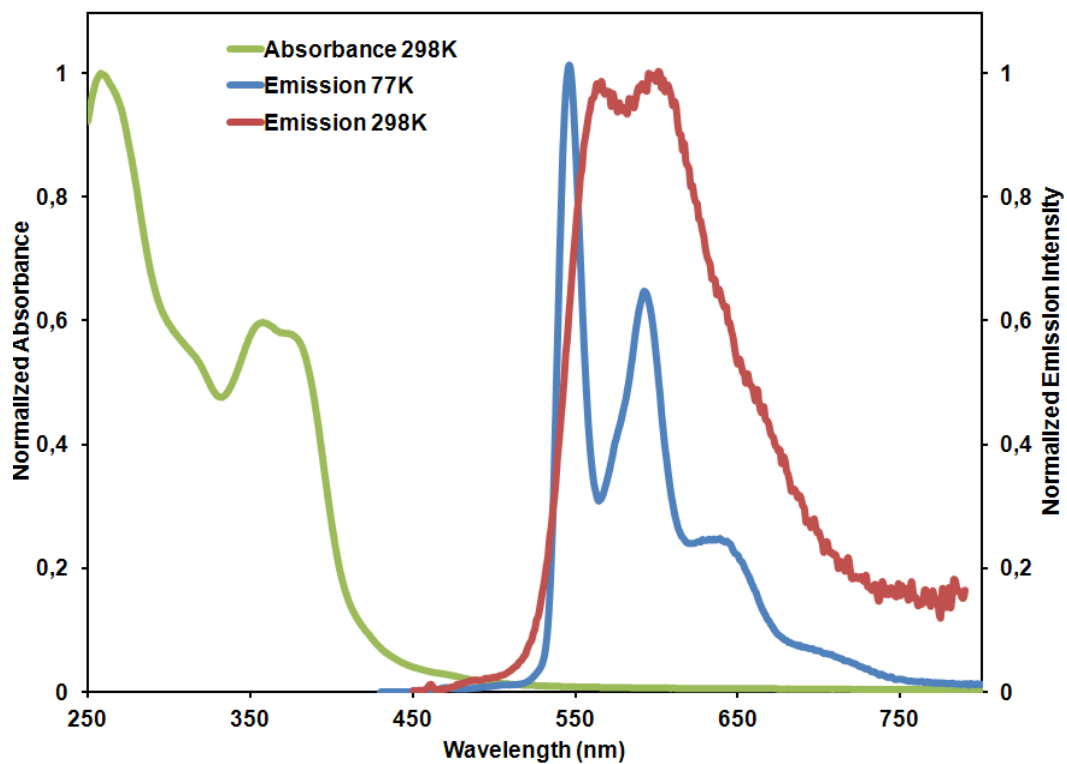


Figure S5: Absorption (green) and emission spectra at 298 K (red) and 77 K (blue) in 2-MeTHF for **3**:

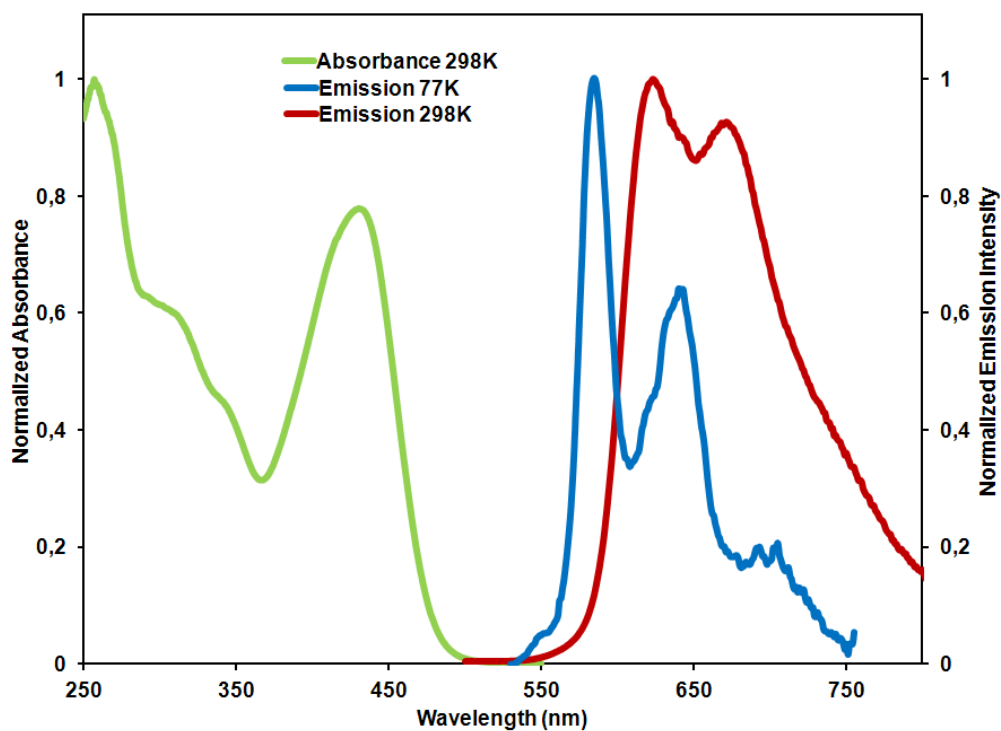


Figure S6: Absorption (green) and emission spectra at 298 K (red) and 77 K (blue) in 2-MeTHF for **5**:

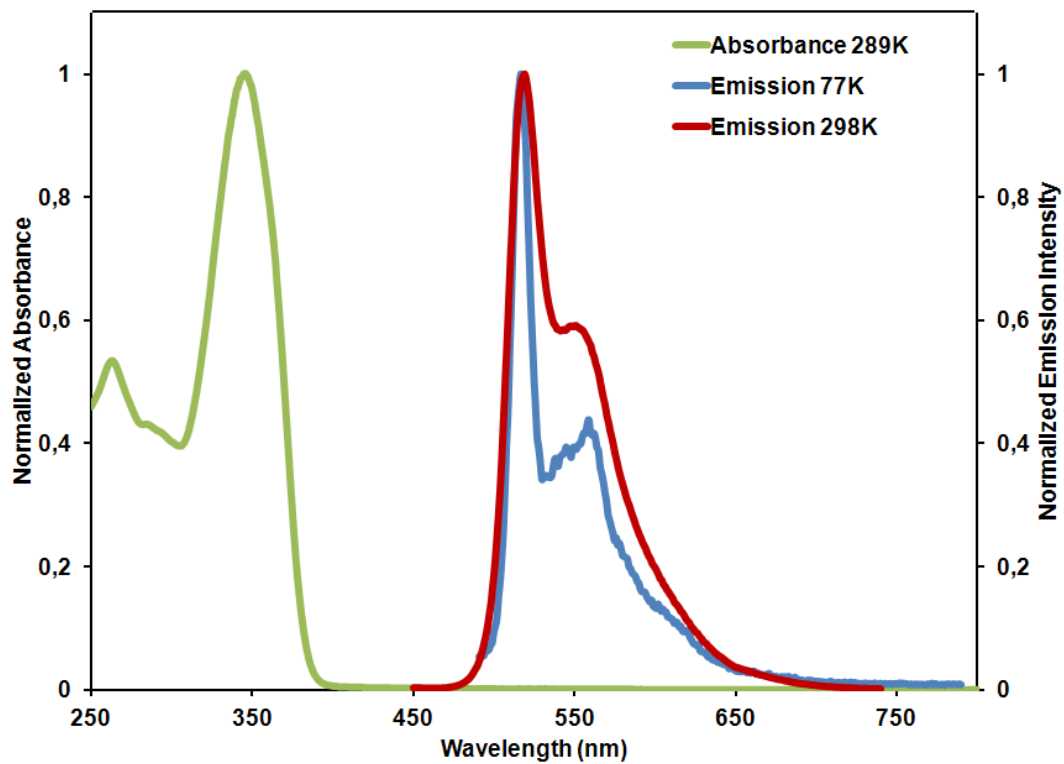


Figure S7: Absorption (green) and emission spectra at 298 K (red) and 77 K (blue) in 2-MeTHF for **6**:

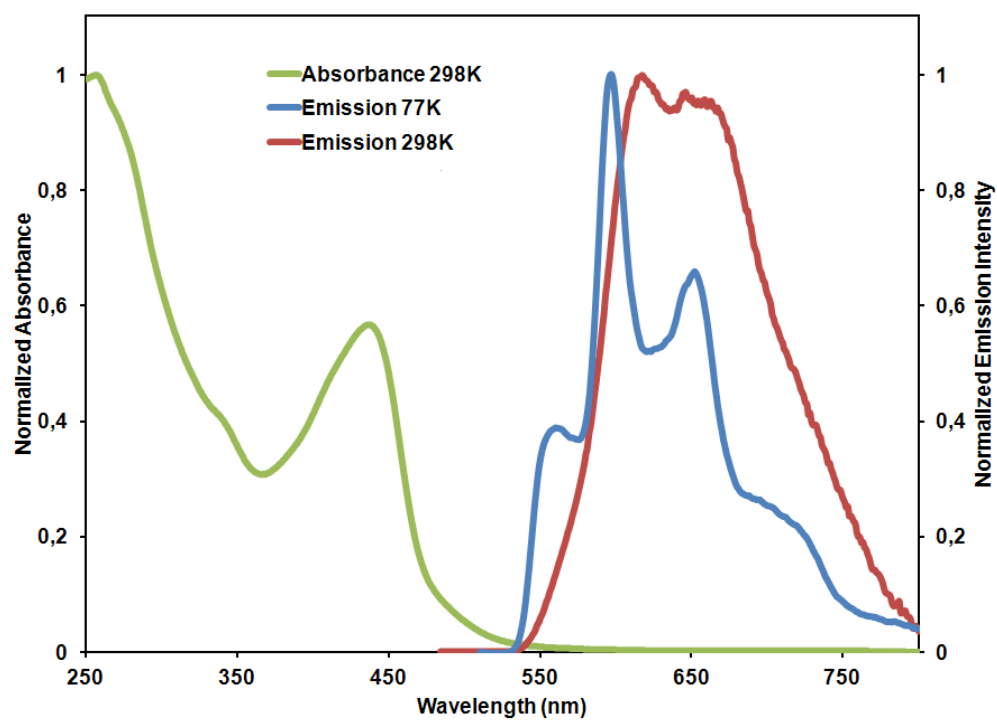


Figure S8: Excitations and absorption at 77K (blue) for **7** in 2-MeTHF:

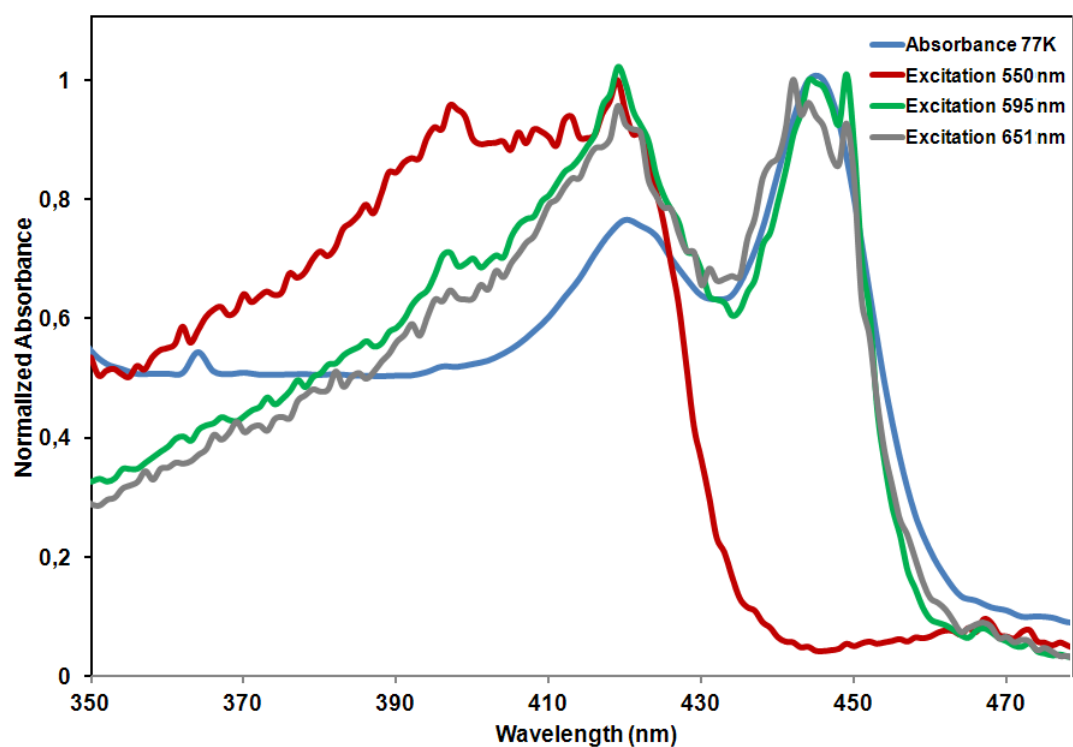
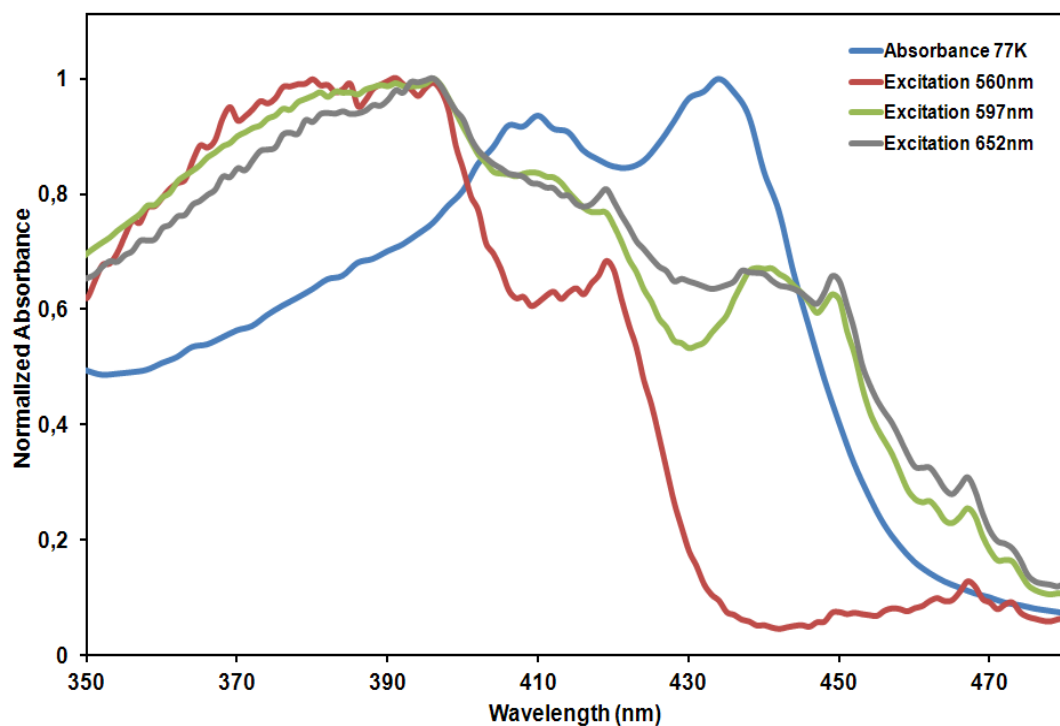


Figure S9: Excitations and absorption at 77K (blue) for **6** in 2-MeTHF:



:

Table S1. Spectroscopic and photophysical data of **1**, **2**, **3**, **6** and **7** in 2-MeTHF:

Complex	Absorbance 298 K (nm) [Molar Absorptivities (x10 ⁴ M ⁻¹ cm ⁻¹)]	Phosphorescence		Stokes shifts		Q.Y. (%) ^a	Lifetime		k _r (x10 ⁵ s ⁻¹)	k _{nr} (x10 ⁵ s ⁻¹)
		77 K (nm)	298 K (nm)	77 K (cm ⁻¹)	298 K (cm ⁻¹)		77 K (μs)	298 K (μs)		
1	260 [3.7]; 315 [2.0]; 390 [1.9]; 450 [0.2]	557	611	7688	9274	8.3	3.4	0.7	0.7	7.6
2	260 [6.8]; 300 [4.1]; 350 [4.0]; 370 [4.0]; 460 [0.2]	547	595	3458	4932	32	11.0	2.9	0.9	2.6
3	260 [4.9]; 310 [2.7]; 345 [1.9]; 425 [4.0]	585	623	6435	7480	4.0	4.7	1.3	0.3	7.2
6	250 [0.3]; 280 [0.2]; 340 [0.1]; 435 [0.2]	558, 596, 654	555, 617, 655	6210	6781	2.6	5.7 (550 nm) 3.3 (650 nm)	1.2	0.21	8.0
7	255 [9.8]; 315 [5.1]; 415 [7.9]; 435 [9.1]	550, 595, 651	560, 613, 663	6182	6675	3.3	2.5 (550 nm) 1.9 (650 nm)	2.3	0.1	3.1

^aMeasured in 2-MeTHF using Ru(bpy)₃(PF₆)₂ Φ = 9.5% in ACN.

Table S2. Cyclic voltammograms for **4**, **2**, **3**, **7** and **6** :

Complex	$E_{1/2ox}$ (V vs SCE)	ΔE_p (mV)	ΔE (V vs SCE)	$E_{1/2red}$ (V vs SCE)	ΔE_p (mV)
4	1.27	60	2.48	-1.21	62
2	1.31	62	2.67	-1.36	56
3	1.36	— ^b	2.71	-1.35	61
7	1.30	50	2.58	-1.27	— ^b
				-1.70	57
6	0.71	— ^b	—	-0.40; -0.77 ^c	— ^b
	1.22	— ^b	—	-0.94; -0.92 ^c	— ^b
	1.34	— ^b	—	-1.30; -1.28 ^c	— ^b

^a Measured in ACN (c.a. 5 mM) with nBu_4NPF_6 (c.a. 1M); scan rate = 200 mV/s. The potentials are reported V vs SCE and were calibrated against an internal standard Fc/Fc^+ (0.40 V in ACN) according to Ref 18;

^b Irreversible; ^c Peak maxima at cathodic and anodic sweeps, respectively.

Table S3. Energy and composition of TD-DFT calculated transitions for **7**:

No.	Energy (cm ⁻¹)	Wavelength (nm)	Oscillator Strength	Symmetry	Major contributions
1	17408.79104	574.422427	0.0001	Singlet-A	HOMO->LUMO (12%), HOMO->L+1 (38%), HOMO->L+2 (49%)
2	17442.66656	573.3068373	0.0001	Singlet-A	H-1->LUMO (17%), H-1->L+1 (57%), H-1->L+2 (24%)
3	18546.8472	539.1751974	0.0007	Singlet-A	H-2->LUMO (87%), H-2->L+2 (10%)
4	20559.2144	486.3999084	0.0001	Singlet-A	HOMO->LUMO (86%), HOMO->L+2 (12%)
5	20722.13952	482.5756525	0.0001	Singlet-A	H-1->LUMO (81%), H-1->L+2 (10%)
6	22179.59344	450.864892	0.0001	Singlet-A	HOMO->L+1 (60%), HOMO->L+2 (38%)
7	22396.55808	446.4971789	0.0123	Singlet-A	H-1->L+1 (33%), H-1->L+2 (65%)
8	22462.696	445.1825373	1.4088	Singlet-A	H-3->LUMO (69%)
9	22845.812	437.7169873	0.05	Singlet-A	H-8->L+1 (24%), H-8->L+2 (15%)
10	22915.98272	436.37666	0.1201	Singlet-A	H-9->L+1 (17%), H-8->L+2 (15%)
11	23133.75392	432.268798	0.0015	Singlet-A	H-6->LUMO (17%), H-2->L+1 (29%), H-2->L+2 (25%)
12	23158.75728	431.8020988	0.0381	Singlet-A	H-7->LUMO (13%), H-6->LUMO (19%), H-2->L+1 (53%)
13	23278.93472	429.5729216	0.0043	Singlet-A	H-6->LUMO (13%), H-2->L+2 (60%)
14	23329.748	428.6372918	0.151	Singlet-A	H-9->LUMO (10%), H-7->LUMO (40%)
15	23406.3712	427.2341028	0.0246	Singlet-A	H-4->LUMO (13%), H-4->L+1 (32%), H-4->L+2 (39%)
16	23440.24672	426.61667	0.0106	Singlet-A	H-5->LUMO (20%), H-5->L+1 (51%), H-5->L+2 (21%)
17	24040.32736	415.9677133	0.0218	Singlet-A	H-9->L+1 (15%), H-7->L+2 (14%), H-6->L+1 (12%), H-3->L+1 (18%), H-3->L+2 (10%)
18	24047.5864	415.8421487	0.1866	Singlet-A	H-7->L+1 (18%), H-7->L+2 (20%), H-6->L+2 (27%)
19	24267.77728	412.0690529	0.6026	Singlet-A	H-15->LUMO (38%)
20	24454.09264	408.9295051	0.034	Singlet-A	H-11->LUMO (78%)
21	24595.24064	406.5827266	0.0054	Singlet-A	H-2->L+3 (74%), HOMO->L+7 (16%)
22	24600.08	406.5027431	0.0439	Singlet-A	H-2->L+3 (22%), HOMO->L+7 (52%), HOMO->L+9 (13%)
23	24762.19856	403.8413623	0.0275	Singlet-A	H-1->L+6 (52%), H-1->L+8 (34%)
24	24905.76624	401.5134449	0.0585	Singlet-A	H-14->L+1 (16%), H-3->L+1 (27%)
25	25151.76704	397.5863797	0.0056	Singlet-A	H-14->L+1 (13%), H-14->L+2 (10%), H-13->L+1 (16%), H-13->L+2 (12%) (16%), H-13->L+2 (12%)

Figure S10: ^1H NMR data for **11**:

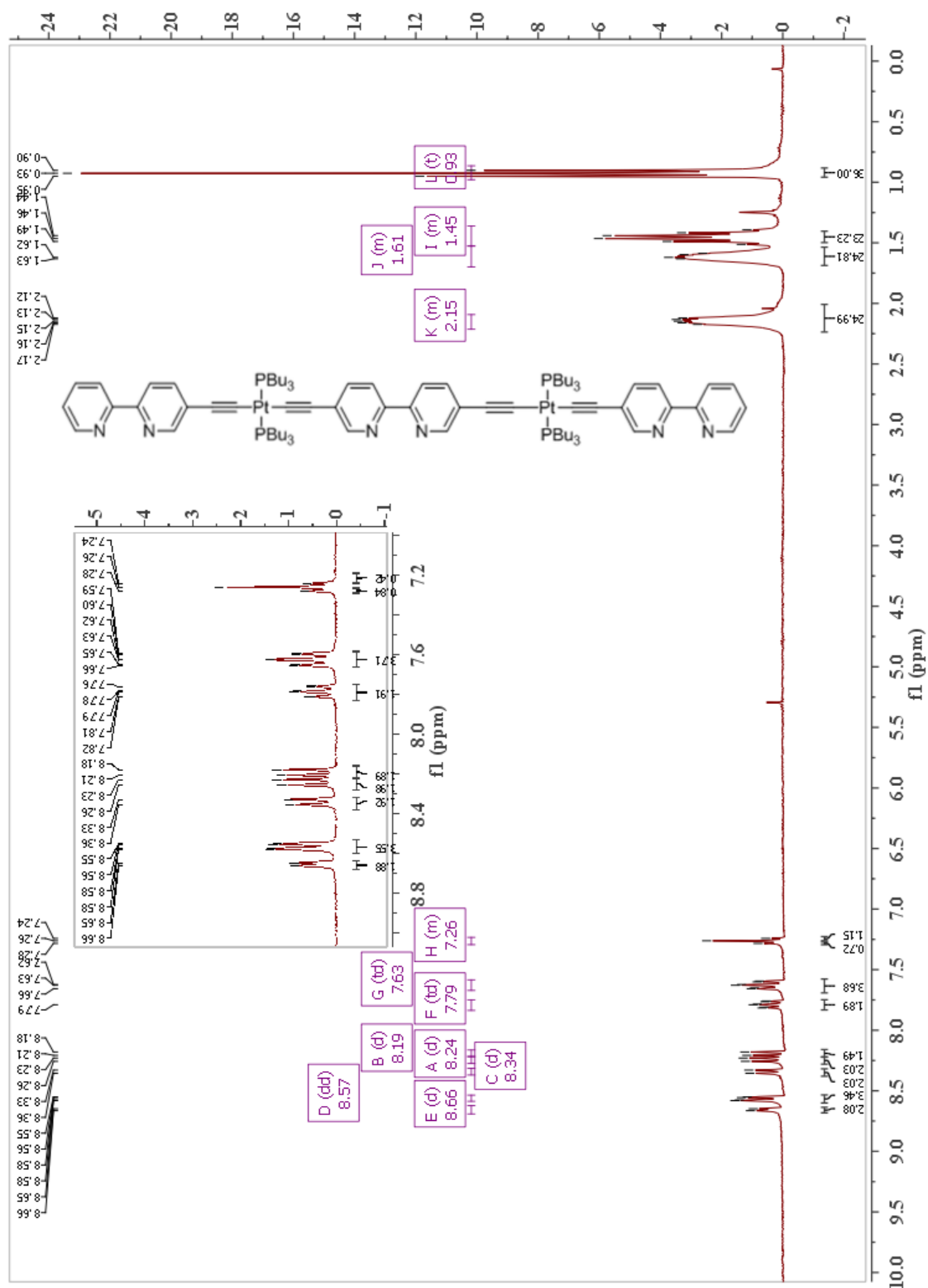


Figure S11: ^{13}C NMR data for **11**:

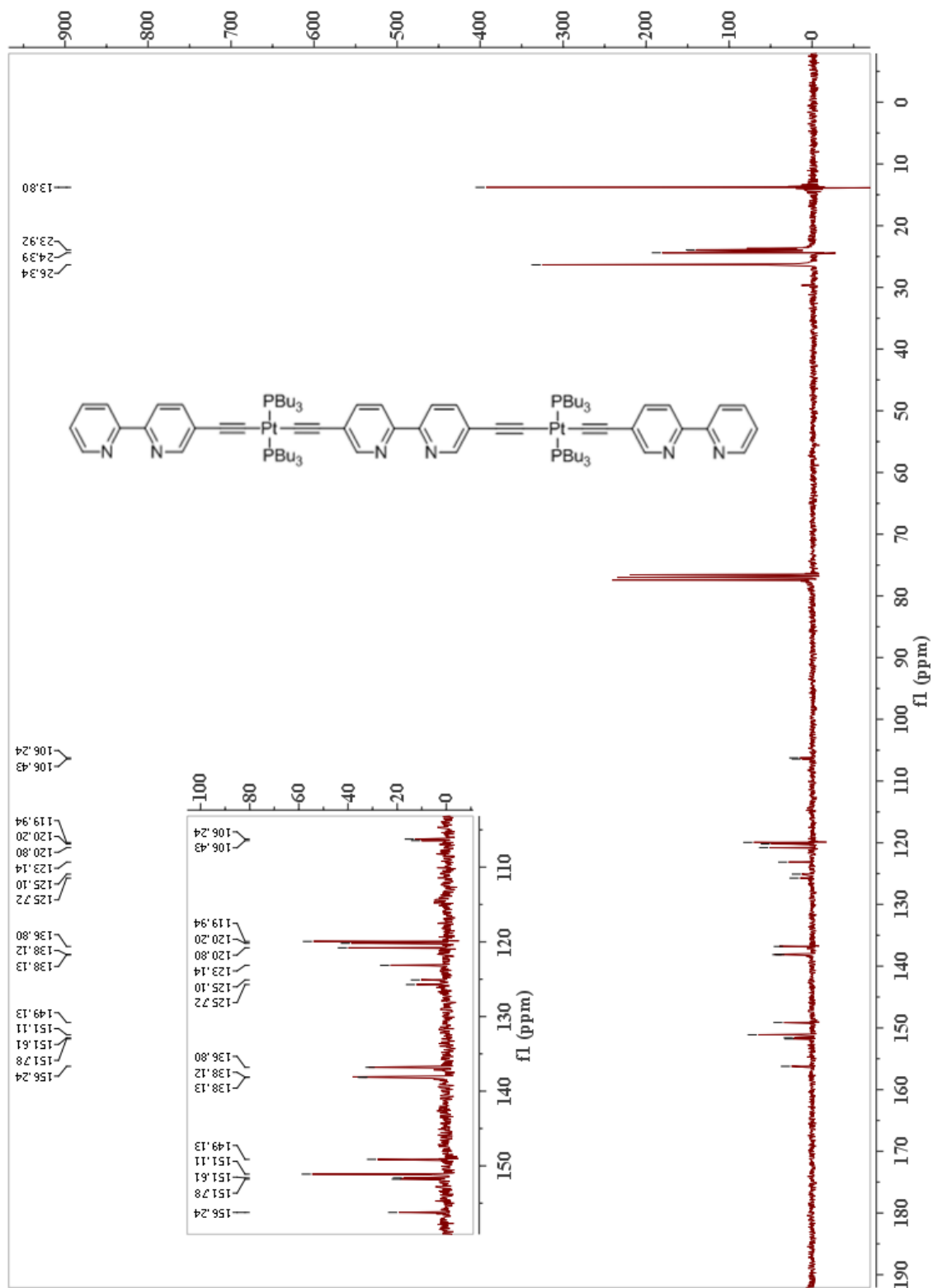


Figure S12: ^{31}P NMR data for **11**:

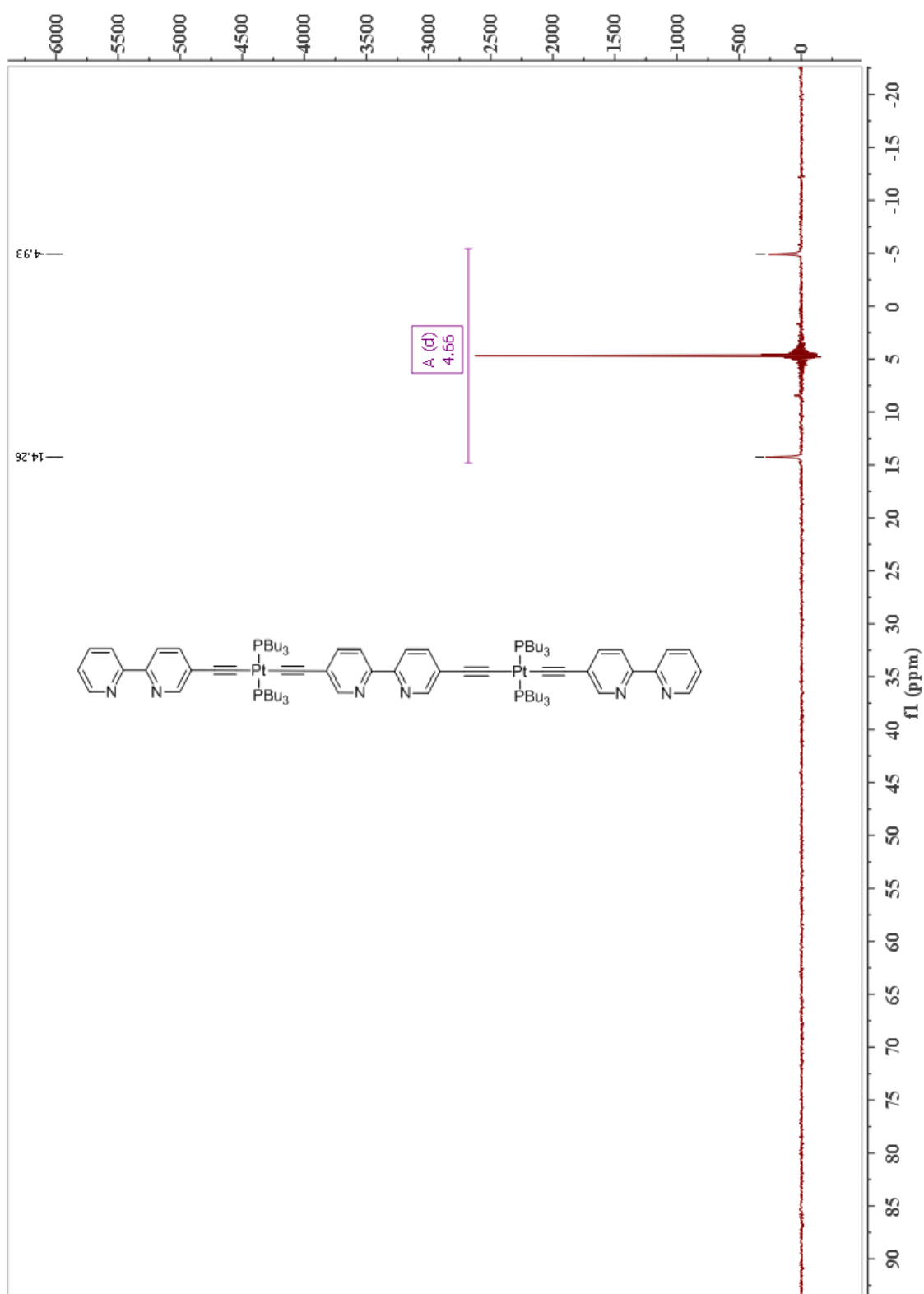


Figure S13: ^1H NMR data for **7**:

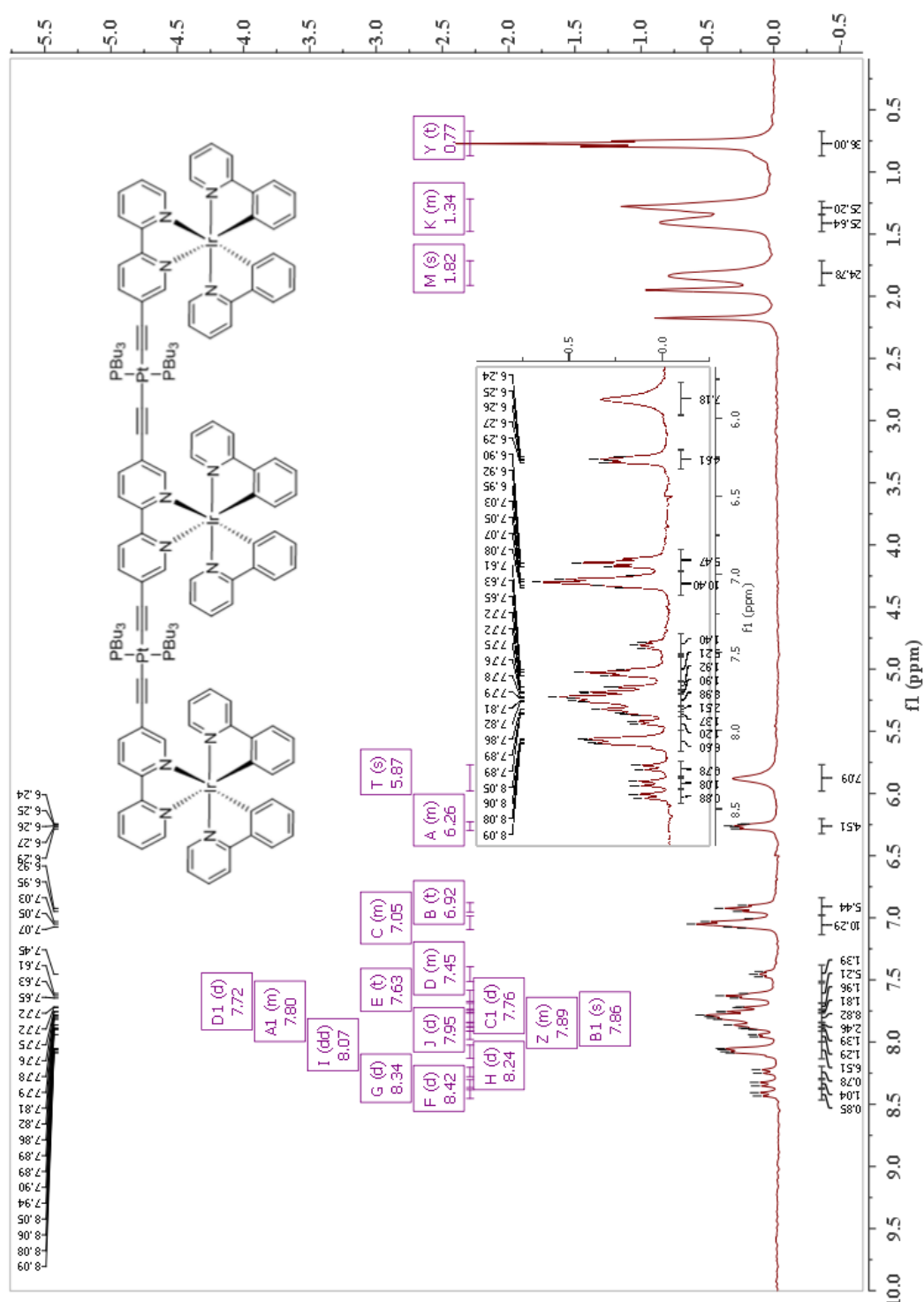
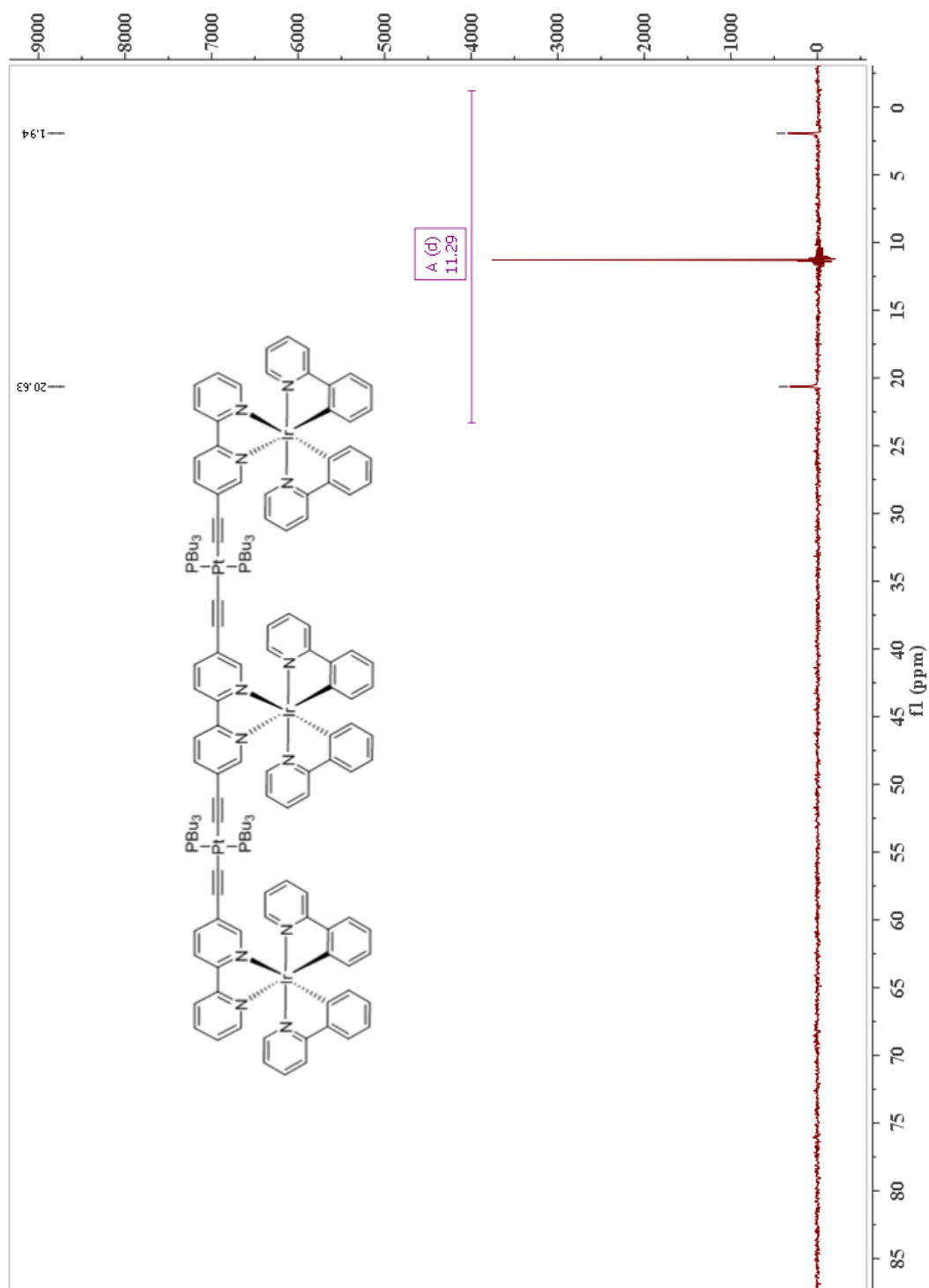


Figure S15: ^{31}P NMR data for **7**:



References:

- (1). G. B. Kauffman, L. A. Teter and J. E. Huheey, in *Inorg. Synth.*, John Wiley & Sons, Inc., 2007, pp. 245-249.
- (2). W. L. F. Armarego and D. D. Perrin, *Purification of Laboratory Chemicals*, 3rd edition, Pergamon Press, Oxford, 1988.
- (3). M. Nonoyama, *Bull. Chem. Soc. Japan*, 1974, **47**, 767.
- (4). S. Ladouceur, A. M. Soliman and E. Zysman-Colman, *Synthesis*, **2011**, 22, 3604.
- (5). A. M. Soliman, D. Fortin, P. D. Harvey, and E. Zysman-Colman, *Chem. Commun.*, **2012**, 48(8), 1120.
- (6). G. A. Crosby and J. N. Demas, *J. Phys. Chem.*, 1971, **75**, 991-1024.
- (7). S. Fery-Forgues and D. Lavabre, *J. Chem. Educ.*, 1999, **76**, 1260.
- (8). H. Ishida, S. Tobita, Y. Hasegawa, R. Katoh and K. Nozaki, *Coord. Chem. Rev.*, 2010, **254**, 2449-2458.
- (9). M. J. Frisch, G. W. Trucks, H. B. Schlegel, G. E. Scuseria, M. A. Robb, J. R. Cheeseman, V. G. Zakrzewski, J. A. Montgomery, R. E. Stratmann, J. C. Burant, S. Dapprich, M. J.M., A. D. Daniels, K. N. Kudin, M. C. Strain, O. Farkas, J. Tomasi, V. Barone, M. Cossi, R. Cammi, B. Mennucci, C. Pomelli, C. Adamo, S. Clifford, J. Ochterski, G. A. Peterson, P. Y. Ayala, Q. Cui, K. Morokuma, A. Malik, A. D. Rabuck, K. Raghavachari, J. B. Foresman, J. Cioslowski, J. V. Ortiz, A. G. Baboul, B. B. Stefanov, G. Liu, A. Liashenko, P. Piskorz, I. Komaromi, R. Gomperts, R. L. Martin, M. Challacombe, P. M. W. Gill, B. G. Johnson, W. Chen, M. W. Wong, J. L. Andres, M. Head-Gordon, E. S. Replogle and J. A. Pople, *Gaussian 98 (Revision A.6)*, Gaussian Inc., Pittsburgh, PA, 1998.
- (10). (a) P. Hohenberg and W. Kohn, *Phys. Rev.*, 1964, **136**, B864; (b) W. Kohn and L. J. Sham, *Phys. Rev.*, 1965, **140**, A1133; (c) in *The Challenge of d and f Electrons*, eds. D. R. Salahub and M. C. Zerner, ACS, Washington, DC, 1989; (d) R. G. Parr and W. Yang, *Density-functional theory of atoms and molecules*, Oxford Univ. Press, Oxford, 1989.
- (11). (a) R. E. Stratmann, G. E. Scuseria and M. J. Frisch, *J. Chem. Phys.*, 1998, **109**, 8218; (b) R. Bauernschmitt and R. Ahlrichs, *Chem. Phys. Lett.*, 1996, **256**, 454; (c) M. E. Casida, C. Jamorski, K. C. Casida and D. R. Salahub, *J. Chem. Phys.*, 1998, **108**, 4439.
- (12). (a) A. D. Becke, *J. Chem. Phys.*, 1993, **98**, 5648-5652; (b) C. Lee, W. Yang and R. G. Parr, *Phys. Rev. B*, 1988, **37**, 785-789; (c) B. Miehlich, A. Savin, H. Stoll and H. Preuss, *Chem. Phys. Lett.*, 1989, **157**, 200-206.
- (13). (a) J. S. Binkley, J. A. Pople and W. J. Hehre, *J. Am. Chem. Soc.*, 1980, **102**, 939; (b) M. S. Gordon, J. S. Binkley, J. A. Pople, W. J. Pietro and W. J. Hehre, *J. Am. Chem. Soc.*, 1982, **104**, 2797; (c) W. J. Pietro, M. M. Francl, W. J. Hehre, D. J. Defrees, J. A. Pople and J. S. Binkley, *J. Am. Chem. Soc.*, 1982, **104**, 5039; (d) K. D. Dobbs and W. J. Hehre, *J. Comp. Chem.*, 1986, **7**, 359; (e) K. D. Dobbs and W. J. Hehre, *J. Comp. Chem.*, 1987, **8**, 861; (f) K. D. Dobbs and W. J. Hehre, *J. Comp. Chem.*, 1987, **8**, 880.
- (14). (a) W. J. Stevens, W. J. Basch and M. Krauss, *J. Chem. Phys.*, 1984, **81**, 6026; (b) W. J. Stevens, M. Krauss, H. Basch and P. G. Jasien, *Can. J. Chem.*, 1992, **70**, 612; (c) T. R. Cundari and W. J. Stevens, *J. Chem. Phys.*, 1993, **98**, 5555-5565.
- (15). (a) M. S. Lowry, W. R. Hudson, R. A. Pascal Jr. and S. Bernhard, *J. Am. Chem. Soc.*, 2004, **126**, 14129-14135; (b) S. Ladouceur, D. Fortin and E. Zysman-Colman, *Inorg. Chem.*, 2010, **49**, 5625-5641.
- (16). N. M. O'Boyle, *GaussSum 2.0*, Dublin City University; Dublin Ireland, 2006.
- (17). J. Tomasi, B. Mennucci and R. Cammi, *Chem. Rev.*, 2005, **105**, 2999-3094.
- (18). Connolly, N. G.; Geiger, W. E. *Chem. Rev.* 1996, **96**, 877.